

Optical spectroscopy and X-ray observations of the D-type symbiotic star EF Aql

K. A. Stoyanov,^{1*} K. Ilkiewicz,² G. J. M. Luna,^{3,4,5} J. Mikołajewska,² K. Mukai,^{6,7} J. Martí,⁸ G. Latev,¹ S. Boeva,¹ and R. K. Zamanov¹

¹*Institute of Astronomy and National Astronomical Observatory, Bulgarian Academy of Sciences, Tsarigradsko Chaussee 72, BG-1784 Sofia, Bulgaria*

²*Nicolaus Copernicus Astronomical Centre, Polish Academy of Sciences, Bartycka 18, P-00716 Warsaw, Poland*

³*CONICET-Universidad de Buenos Aires, Instituto de Astronomía y Física del Espacio (IAFE), Av. Inte. Güiraldes 2620, C1428ZAA, Buenos Aires, Argentina*

⁴*Universidad de Buenos Aires, Facultad de Ciencias Exactas y Naturales, Buenos Aires, Argentina*

⁵*Universidad Nacional de Hurlingham, Av. Gdor. Vergara 2222, Villa Tesei, Buenos Aires, Argentina*

⁶*CRESST and X-ray Astrophysics Laboratory, NASA Goddard Space Flight Center, Greenbelt, MD 20771, USA*

⁷*Department of Physics, University of Maryland, Baltimore County, 1000 Hilltop Circle, Baltimore, MD 21250, USA*

⁸*Departamento de Física (EPSJ), Universidad de Jaén, Campus Las Lagunillas, A3-420, 23071, Jaén, Spain*

Accepted 2020 May 5. Received 2020 May 5; in original form 2020 February 13

ABSTRACT

We performed high-resolution optical spectroscopy and X-ray observations of the recently identified Mira-type symbiotic star EF Aql. Based on high-resolution optical spectroscopy obtained with SALT, we determine the temperature ($\sim 55\,000$ K) and the luminosity ($\sim 5.3 L_{\odot}$) of the hot component in the system. The heliocentric radial velocities of the emission lines in the spectra reveal possible stratification of the chemical elements. We also estimate the mass-loss rate of the Mira donor star. Our *Swift* observation did not detect EF Aql in X-rays. The upper limit of the X-ray observations is 10^{-12} erg cm⁻² s⁻¹, which means that EF Aql is consistent with the faintest X-ray systems detected so far. Otherwise we detected it with the UVOT instrument with an average UVM2 magnitude of 14.05. During the exposure, EF Aql became approximately 0.2 UVM2 magnitudes fainter. The periodogram analysis of the V-band data reveals an improved period of 320.4 ± 0.3 d caused by the pulsations of the Mira-type donor star.

The spectra are available upon request from the authors.

Key words: stars: binaries: symbiotic – stars: AGB and post-AGB – accretion, accretion discs – stars: individual: EF Aql

1 INTRODUCTION

EF Aquilae was identified as a variable star on photographic plates from Königstuhl Observatory (Reinmuth 1925). Richwine et al. (2005) have examined the optical photometry for EF Aql and classify it as a Mira-type variable with a period of 329.4 d and amplitude of variability > 2.4 mag in V band. Margon et al. (2016) reported that it has bright UV flux, prominent Balmer emission lines, and [O III] $\lambda 5007$ emission. Thus EF Aql is classified as a symbiotic star, belonging to the symbiotic Mira subgroup. Zamanov et al. (2017) showed that EF Aql displays flickering (stochastic variability with amplitude ~ 0.2 magnitudes on a time scale of ~ 20 minutes) in B and V bands, which

is a rarely detectable phenomena among the symbiotic stars (Sokoloski et al. 2001).

Symbiotic stars are long-period interacting binaries, consisting of an yellow or red giant transferring mass to a hot compact object. According to the classification of Webster & Allen (1975), the symbiotic stars are divided into two types – those with cool stellar continuum (S-type) and those with infrared excess from dust (D-type). The D-type symbiotics have near-IR variations that are caused by the presence of a thermally pulsating Mira-type variable, while in S-type symbiotic stars a normal red giant is present. Allen (1982) introduced D'-type symbiotic stars, in which dust is present and a cool giant of spectral type F or G is the donor. The orbital periods of the symbiotic stars are in the range of 100 days to more than 100 years (Gromadzki et al.

* E-mail: kstoyanov@astro.bas.bg

Table 1. UBVR_{CIC} photometry of EF Aql obtained on 2019-07-06.

date	band	mag
2019-07-06 01:49	U	14.46 ± 0.08
2019-07-06 01:52	B	15.41 ± 0.06
2019-07-06 01:56	B	15.53 ± 0.07
2019-07-06 01:58	V	14.92 ± 0.06
2019-07-06 01:59	V	14.96 ± 0.05
2019-07-06 01:55	R	14.06 ± 0.03
2019-07-06 02:00	R	13.97 ± 0.03
2019-07-06 01:56	I	11.25 ± 0.03
2019-07-06 02:00	I	11.28 ± 0.03

2013). The D-type symbiotics have longer orbital periods (Hinkle et al. 2013), because the orbits need to be wide enough to harbour a Mira variable with a diameter of several AU and a mass of $\sim 1 - 3 M_{\odot}$ (Vassiliadis & Wood 1993). In most symbiotic stars, the secondary is a hot and luminous accreting white dwarf (Mikołajewska 2012). In a few cases has the secondary been shown to be a neutron star (Davidsen et al. 1977; Kuranov & Postnov 2015). The whole symbiotic system is surrounded by a circumstellar nebula formed by the matter lost from the components.

2 OBSERVATIONS

2.1 Photometry

The V-band light curve of EF Aql based on data from ASAS (Pojmanski 1997), ASAS-SN (Shappee et al. 2014; Kochanek et al. 2017) and AAVSO International database is shown on Fig.1. In addition, a UBVR_{CIC} photometric series of EF Aql were obtained in the period 2016 – 2019 with the 50/70 cm Schmidt telescope of the Rozhen National Astronomical Observatory, Bulgaria. Journal of UBVR_{CIC} observations, obtained on 2019 July 06, is given in Table 1.

2.2 SALT observations

Spectroscopic observations were carried out on 2019 June 07, 2019 July 09 and 2019 July 14 with the 11m Southern African Large Telescope (Buckley et al. 2006; O’Donoghue et al. 2006) using the High Resolution Spectrograph (Bramall et al. 2010, 2012; Crause et al. 2014). The time of observations corresponds to phases $\Phi=0.61$, $\Phi=0.71$ and $\Phi=0.72$ respectively (for details see Section 3.1). The exposure times are 1900 s. The spectrograph was used in a medium resolution mode with resolving power $R \sim 40000$ and wavelength coverage of 4000 – 8800 Å. The initial data reduction was performed using pysalt pipeline (Crawford et al. 2010) which was followed by HRS pipeline (Kniazev et al. 2017), based on MIDAS feros (Stahl et al. 1999) and echelle (Ballester 1992) packages. In Table 2 we present the measured equivalent widths (EWs), full widths at half maximum (FWHMs) and heliocentric radial velocities (RV_{hel}) of some emission lines in the spectrum of EF Aql. The measurements are done by employing a Gaussian fit. Figures 2 and 3 show the regions around the H α and H β emission lines.

2.3 Swift observations

X-ray and UV observations were obtained using the *Neil Gehrels Swift observatory* (hereafter *Swift*) on 2019-09-12 (ObsID: 00011552001). The X-Ray Telescope (XRT) was operated in photon counting mode, while the UltraViolet and optical Telescope (UVOT) was operated in imaging mode using UVM2 filter, centered approximately at 2200 Å, and both achieved a total exposure of approximately 3.8 ksec.

3 RESULTS

3.1 Period of pulsations

Using the photometric data, we performed periodogram analysis in order to confirm and improve the detected period of 329.4 d, that is associated with the pulsations of the Mira-type donor star (Richwine et al. 2005). Using the CLEAN algorithm (Roberts et al. 1987), PDM method (Stellingwerf 1978) and Fourier transform we obtained periods of 321.2 ± 0.1 d, 320.8 ± 0.1 d and 320.4 ± 0.3 d respectively. We present the periodograms of the CLEAN and PDM methods on Fig.4. The period and the amplitude of the pulsations (~ 4 mag, see Fig.1) are typical for the Mira-type variables (Whitelock et al. 2003). For the purposes of our study, we use the following ephemeris:

$$JD_{max} = (2458127.3 \pm 1.6) + (320.4) \pm 0.3 \times E \quad (1)$$

We present the V-band light curve of EF Aql folded with the period of 320.4 d on Fig.5.

3.2 Distance and interstellar reddening

As Le Bertre et al. (2003) classified EF Aql as an O-rich star, we could use the period – luminosity relations for Miras for estimation of the distance to the object (Whitelock et al. 2008):

$$M_K = \rho[\log P - 2.38] + \delta \quad (2)$$

where $\rho = -3.51 \pm 0.20$ and $\delta = -7.25 \pm 0.07$ (Gromadzki et al. 2009). We derive mean K-band magnitude from 2MASS All Sky Catalog and DENIS database $K=4.78 \pm 0.58$ and absolute K-band magnitude, $M_K = -7.69$ obtained using Eq. 2. In Zamanov et al. (2017) we assumed interstellar extinction $E(B-V)=0.45$, which seems very overestimated. The NASA/IPAC IRSA (Galactic Reddening and Extinction Calculator) gives low extinction through our galaxy in the direction of EF Aql, $E(B - V) < 0.17$, so the extinction in K-band should be insignificant. From these magnitudes we estimate the distance to EF Aql to be $d = 3.1$ kpc.

In order to estimate the interstellar plus circumstellar extinction, we compare the observed and intrinsic $J-K$ colours. Using the period – colour relation by Whitelock et al. (2000) for O-rich Miras:

$$(J - K)_0 = 0.71 \log P - 0.39. \quad (3)$$

The 2MASS All Sky Catalog and DENIS database give observed $J-K$ colours 1.61 and 1.81 respectively, which corresponds to $E(J-K) = 0.32 \pm 0.10$.

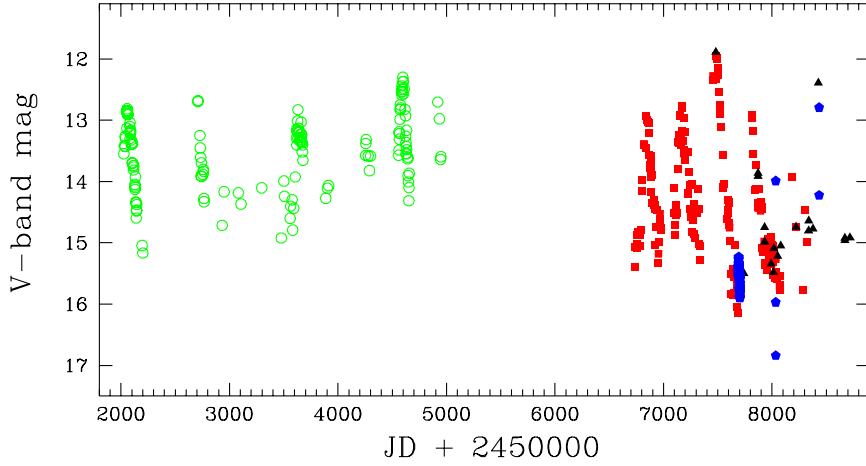


Figure 1. The V-band photometric observations of EF Aql. The green open circles represent the data from ASAS, the red squares – the ASAS-SN data, the blue pentagons – the AAVSO data and the black triangles are the observations from Rozhen NAO.

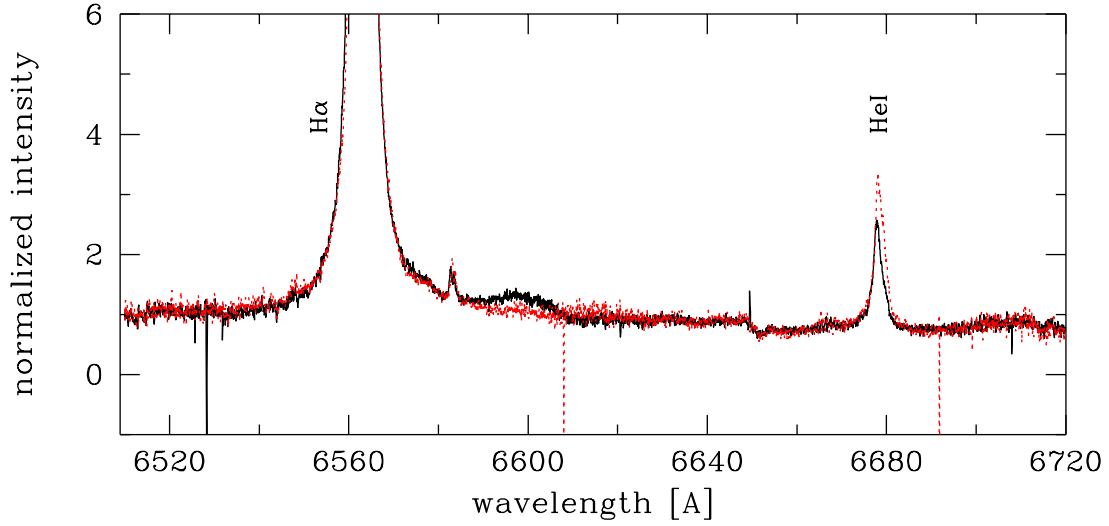


Figure 2. The region around $H\alpha$ in the spectrum of EF Aql. Black solid line is 2019-06-07, red dashed line – 2019-07-14.

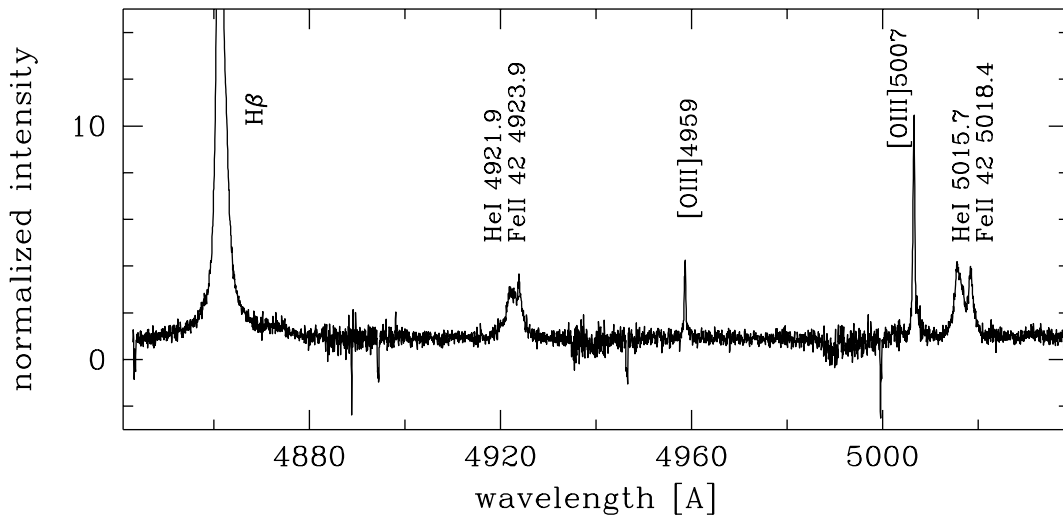
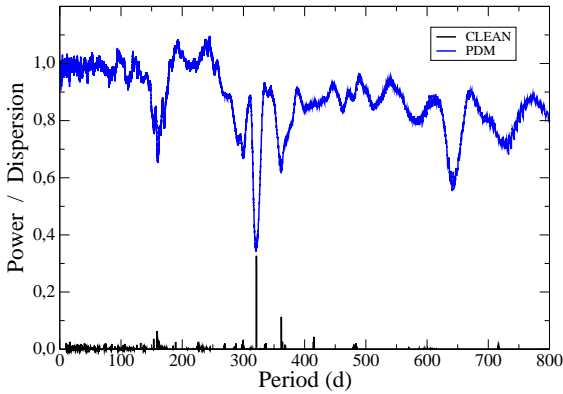


Figure 3. The emission lines around the $H\beta$ line in the spectrum of EF Aql.

Table 2. The measured EWs, FWHMs and heliocentric velocities of the lines in the spectrum of EF Aql. Negative values of EWs denote emission lines, while positive values denote absorption lines.

line	2019-06-07			2019-07-09			2019-07-14		
	EW [Å]	FWHM [km s ⁻¹]	RV _{hel} [km s ⁻¹]	EW [Å]	FWHM [km s ⁻¹]	RV _{hel} [km s ⁻¹]	EW [Å]	FWHM [km s ⁻¹]	RV _{hel} [km s ⁻¹]
H α 6562.82	-88.40	83	3.4	-90.7	74	2.8	-88.8	74	1.0
H β 4861.33	-11.37	85	0.8	-10.4	60	-0.8	-11.4	59	-3.1
H γ 4340.47	-2.78	58	-2.1	-1.51	44	-3.7	-3.27	44	-3.2
HeI 4471.48	-1.46	63	7.9	-1.34	71	-2.1	–	–	–
HeI 4713.14	-0.1	38	12.3	-0.06	37	3.5	-0.08	15	-0.8
HeI 4921.93	-1.33	91	16.2	-2.92	152	17	-3.80	120	15.9
HeI 5015.68	-2.57	115	19.3	-3.72	132	12	-5.94	130	21
HeI 5875.64	-3.19	67	2.4	-3.31	53	-11.9	-2.07	39	-2.9
HeI 6678.15	-0.95	48	6.3	-0.30	28	-2.5	-0.50	33	-2.1
HeI 7065.19	-1.66	52	1.5	-0.90	32	-0.8	-1.40	35	-1.4
[OIII] 4363.21	-0.37	41	-6.3	-0.39	34	-7.8	-0.52	32	-6.0
[OIII] 4958.92	-0.75	25	-12.2	-0.99	27	-10.9	-1.29	25	-12.0
[OIII] 5006.85	-1.66	25	-11.9	-1.57	26	-12.0	-2.56	28	-12.5
[OI] 8446.60	-2.69	60	2.2	–	–	–	-1.32	42	-2.3
FeII 38 4549.47	-0.92	63	-0.5	-0.24	36	3.4	–	–	–
FeII 38 4583.83	-0.71	52	4.9	-0.58	50	0.8	-0.54	49	7.0
FeII 37 4629.34	-0.82	90	6.9	-0.58	110	17.2	-0.89	67	3.7
FeII 42 4923.92	-1.95	79	3.4	-1.18	64	12.7	-2.68	88	8.6
FeII 42 5018.43	-1.84	67	4.9	-1.92	74	8.4	-2.61	69	7.3
[NII] 6583.29	-0.41	38	-11.2	-0.31	34	-13.7	-0.27	27	-5.4
NaI D1 5889.95	0.45	19	-15.8	0.31	14	-16.7	0.33	16	-12.8
NaI D2 5895.92	–	–	–	0.29	15	-16.4	0.24	13	-13.0

**Figure 4.** Periodograms for the V-band magnitude of EF Aql computed using the CLEAN and PDM algorithms. The period of pulsations of the Mira is detected as the most significant one.

In our spectra we do not detect DIB 6613 Å. No interstellar component is visible in KI 7699 line (see Fig.6). The NaI D lines shows complex profiles with a moderately broad emission and at least two narrow absorption components. The stronger blue absorption component may be of local origin, e.g. circumstellar material, while the red component is of interstellar origin. The EW of the Na D1 line is in the range 0.31 Å – 0.45 Å which corresponds to E(B-V)=0.12 – 0.25

(Munari & Zwitter 1997). It is possible that E(J-K) represents the total (circumstellar and interstellar) extinction and E(B-V) marks only the interstellar extinction. This would indicate significant circumstellar reddening, as expected for a D-type symbiotic systems (Gromadzki et al. 2009).

3.3 Temperature and luminosity of the hot component

The minimum temperature is set by the maximum ionization potential observed in the spectrum which in our case is 35.12 eV corresponding to the [OIII] lines (Peterson 1997). This gives a temperature $T_{hot} \gtrsim 35\,000$ K. The lack of any traces of HeII lines and the presence of strong HeI lines means that $T_{hot} \lesssim 60\,000$ K.

Using the photometric observations listed in Table 1, we estimate:

$$F_{cont}(R) \sim F_{cont}(6580 \text{ \AA}) \sim 5.6 \times 10^{-15} \text{ erg s}^{-1} \text{ cm}^{-2} \quad (4)$$

This in combination with the measured EW of the H α line (see Table 2) gives total flux in the H α line: $F(\text{H}\alpha) \sim 9 \times 10^{-13} \text{ erg s}^{-1} \text{ cm}^{-2}$.

Following the same pattern for the V-band magnitude and the HeI 5876 Å line, and the B-band magnitude and

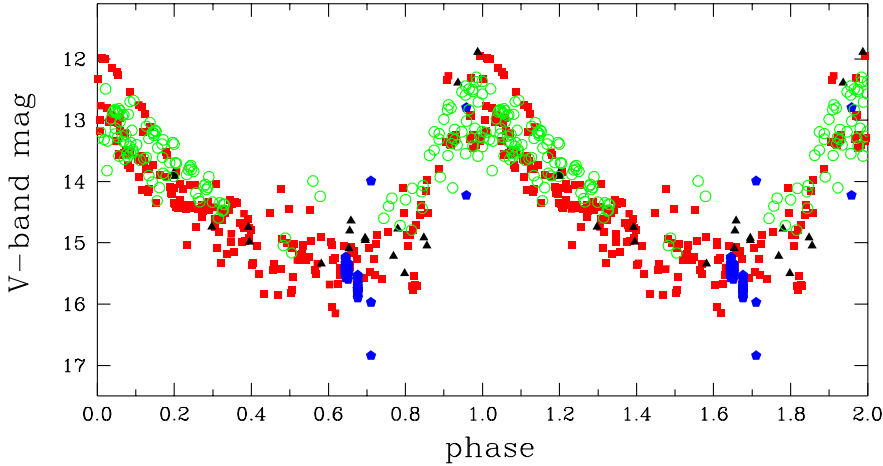


Figure 5. The V-band photometric observations of EF Aql folded with the period of the pulsations. The symbols are the same as on Fig.1.

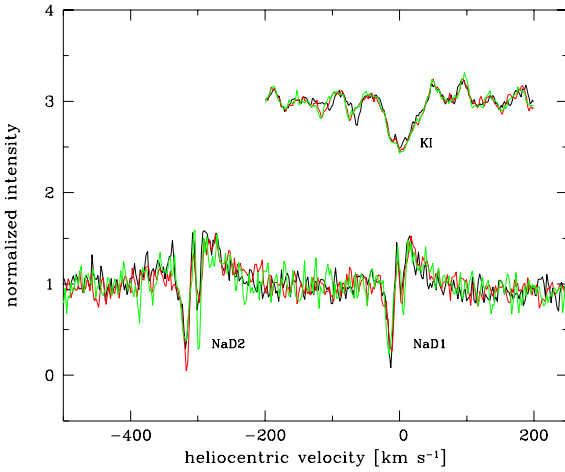


Figure 6. The spectra of EF Aql in NaD1 and KI7699 lines. Black solid line is 2019-06-07, red dashed line – 2019-07-09, green – 2019-07-14. Sharp interstellar absorptions are visible in NaD1 and NaD2 lines. No interstellar component is visible in KI 7699.

the $H\beta$ lines, the total fluxes in the lines are:

$$F(\text{HeI } 5876) \sim 4 \times 10^{-14} \text{ erg s}^{-1} \text{ cm}^{-2}.$$

$$F(H\beta) \sim 1.2 \times 10^{-13} \text{ erg s}^{-1} \text{ cm}^{-2}.$$

Assuming photonization, case B recombination (Netzer 1975) and blackbody ionizing source/hot component, the ratio $F(\text{HeI } 5876)/F(H\beta)$ indicates $T_{\text{hot}} \sim 55\,000$ K, and the total $H\beta$ and HeI 5876 fluxes imply a hot component luminosity $L_{\text{hot}} \sim 5.3 L_{\odot}$ using $d = 3.1$ kpc.

3.4 Mass-loss rate

The Mira pulsations play a crucial role in the mass-loss process because they raise the dense material from the atmosphere to distances where the temperature is too low to form dust grains. This is not a well-understood process on the case of the O-rich Miras. It is believed that a combination of the stellar pulsation and radiation pressure on dust is not enough to drive the mass loss (Woitke 2006) and the proper mechanism is a subject of debates.

To estimate the mass loss for EF Aql, we use the correlation between the mass-loss rate and the K-[12] colour for O-rich Mira variables. The K and [12] fluxes originate from the star and the dust shell respectively, so larger K-[12] colour means thicker shell. Therefore, the K-[12] colour provides a useful tool for mass-loss rate estimation. Using the mean K-band magnitude (see Sect. 3.2) and the flux at $12 \mu\text{m}$ provided by IRAS database (Neugebauer et al. 1984), we estimate $K-[12] = 2.89$. Using Fig.21 from Whitelock et al. (1994), we estimate the mass-loss rate for EF Aql to be $\sim 2.5 \times 10^{-7} M_{\odot} \text{ yr}^{-1}$. The mass-loss rates of the single O-rich Miras are in the range from $10^{-7} M_{\odot} \text{ yr}^{-1}$ to $10^{-5} M_{\odot} \text{ yr}^{-1}$ (Whitelock et al. 1994). The Miras in the symbiotic systems have an average mass-loss rate $\sim 3.2 \times 10^{-6} M_{\odot} \text{ yr}^{-1}$ (Gromadzki et al. 2009). The measured low value for EF Aql is in agreement with our considerations for a low-luminosity system (see the Discussion section).

3.5 X-ray and UV emission

Our *Swift* observation did not detect EF Aql in X-rays, with an upper limit of 0.003 c s^{-1} . Assuming an absorbing column of 10^{23} cm^{-2} and a plasma temperature of 10 keV (typical of δ component in symbiotics), this upper limit on the count rate translates into an unabsorbed flux of $10^{-12} \text{ erg cm}^{-2} \text{ s}^{-1}$ and into a luminosity of about half a solar luminosity. This upper limit is consistent with the faintest δ components detected so far (the component from the boundary layer between the accretion disc and the white dwarf; Luna et al. (2013)). In turn, we detected EF Aql with the UVOT instrument onboard *Swift*, with an average UVM2 magnitude of 14.05 (uncorrected for reddening). During the 25 ks that *Swift* was pointing to EF Aql, we observed that it got approximately 0.2 UVM2 magnitudes fainter. We can only speculate about this behavior, which could be due to variable absorption and/or flickering from the accretion disk.

4 DISCUSSION

The Balmer lines show complex profiles with a relatively broad and a narrow component (Fig. 7). The same struc-

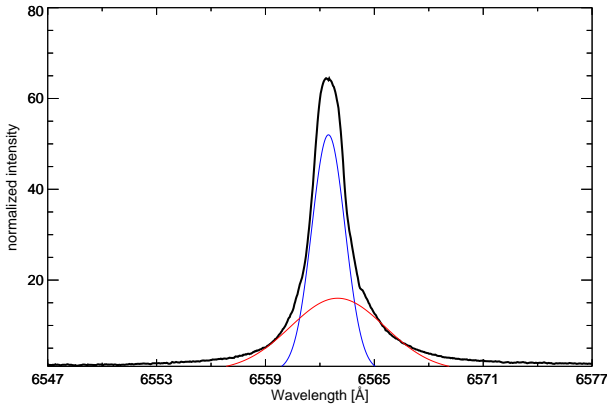


Figure 7. The broad and narrow components of the $H\alpha$ line fitted with two Gaussians with FWHMs $\sim 1.8 \text{ \AA}$ and 6.0 \AA respectively.

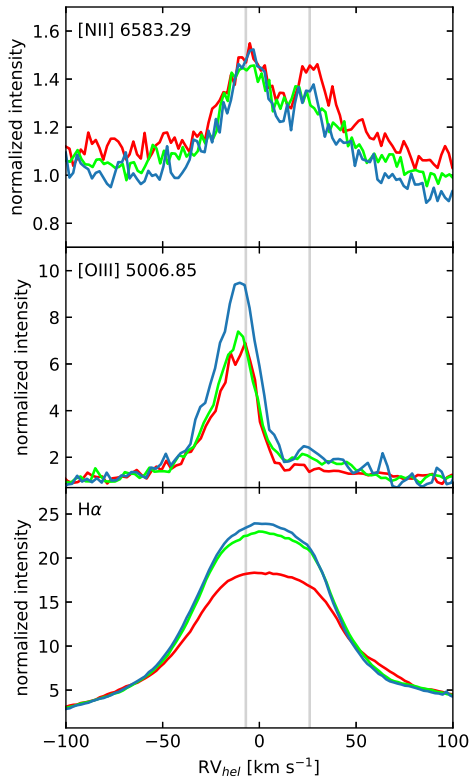


Figure 8. Comparison of emission lines profiles of EF Aql. The gray lines indicate the positions of two maxima in the [NII] 6583.29 line. Red line: SALT 2019.06.06 spectrum, green line: SALT 2019.07.09 spectrum, blue line: SALT 2019.07.13 spectrum.

ture is present in the strongest HeI lines (4471 \AA , 4713 \AA , 5876 \AA , 6678 \AA and 7065 \AA) while it is less obvious in the fainter lines. In the case of HeI 4922 and HeI 5016 the nearby FeII lines may hide the fine structure of the HeI lines (Fig. 3). No HeII lines are detected in the spectra.

The [NII] 6583 line seems to have double-peaked structure with the red component 50 – 60% of the blue

one (Fig. 8) The same profile appears on all spectra. In the case of [OIII] lines, only the blue component is visible. The line profile is very similar to that in planetary nebulae (Lutz et al. 1989) and it may be originate in a faint fossil nebula ejected by the present white dwarf component during its AGB stage (Munari & Patat 1993).

It is also interesting that the $H\alpha$ profile appears to have flat top, and, in principle, the narrow component may consist of two narrow lines with velocity separation similar to that found in [NII] profiles.

The temperature of the hot components in symbiotics is in the range $35\,000 \text{ K} - 500\,000 \text{ K}$ and the luminosity is in the range $0.3 L_{\odot} - 37\,000 L_{\odot}$ (Muerst et al. 1991; Muerst & Nussbaumer 1994; Mikolajewska et al. 1997; Orio et al. 2007). Mikolajewska et al. (1997) found that the temperature of the hot component correlates with the Raman scattered $\lambda 6825$ line. The 6825 \AA emission is produced due to Raman scattering of O VI $\lambda 1032$ by hydrogen atoms (Schmid 1989). The lack of $\lambda 6825$ emission in EF Aql supports our result for a hot component with low luminosity.

The typical red giant in symbiotic system have a mass-loss rate of $\sim 10^{-7} M_{\odot} \text{ yr}^{-1}$, which is enough to power a luminosity of $10 - 100 L_{\odot}$. In systems with hydrogen shell burning on the surface of the white dwarf, even an accretion rate of $\sim 10^{-8} M_{\odot} \text{ yr}^{-1}$ can produce that amount of luminosity. The Mira-type variables have a mass loss rate of $\sim 10^{-5} M_{\odot} \text{ yr}^{-1} - 10^{-7} M_{\odot} \text{ yr}^{-1}$ (Whitelock et al. 1994), but the larger distance between the components in the D-type symbiotic stars results similar luminosities. In the systems without hydrogen shell burning on the surface of the white dwarf (the case of EF Aql), the luminosity of the hot component is more or less equal to that generated by the accretion (Paczynski & Zytkow 1978).

The obtained parameters set up EF Aql among the systems with lowest temperature and luminosity of the hot component and the most probable reason is the low accretion rate.

The AGB stage is the final stage of the evolution of the low- and intermediate-mass stars before they turn into white dwarfs. The evolution during this stage is driven by a large range of complex processes, including the stellar pulsations and the mass loss. The AGB stars can reach mass-loss rates so high that mass loss process can determines the evolutionary time scales, instead of nuclear burning time scale. Large-scale convective flows bring newly-formed chemical elements from the stellar interior to the surface and, boost by the stellar pulsations, they trigger shock waves in the extended stellar atmosphere, where they formed massive outflows of gas and dust. These outflows not only enrich the interstellar medium, but also play a crucial role in the evolution of the cool giant into a white dwarf (Höfner & Olofsson 2018). The progenitors of the short-period Miras have a mass of $1.0 - 1.1 M_{\odot}$ (Jura 1994), while the Miras with periods in the range $400 - 600 \text{ d}$ have progenitors with masses $\geq 2 M_{\odot}$. The lifetime of a star with initial mass $1 - 2 M_{\odot}$ during the AGB stage is in the range $1 - 3 \times 10^6 \text{ yr}$ (Kalirai et al. 2014). For a Mira

with period ~ 300 d, we should expect an increase of the period and the mass loss (Trabucchi et al. 2019). Following these considerations, for the future evolution of EF Aql we are expecting an increase of the accretion rate onto the white dwarf followed by an increase of the X-ray activity but the evolution of EF Aql in general should be considered in terms of the binary evolution.

EF Aql appears to be powered by accretion onto a white dwarf without shell nuclear burning on the surface of the white dwarf. The presence of optical flickering (Zamanov et al. 2017) and the modest hot component luminosity (this work) are both consistent with this interpretation. While we did not detect EF Aql in X-rays, particularly X-rays of the δ -type (Luna et al. 2013), our upper limit is still consistent with lower-luminosity end of accretion-powered symbiotics.

The measured heliocentric radial velocities (see Table 2) point for a possible ionization potential dependent stratification in EF Aql. Similar effect is detected in the D-type symbiotic RR Tel (Kotnik-Karuza et al. 2004) and in some S-type symbiotic stars (Friedjung et al. 2010). A velocity stratification of various spectral lines is also detected in some Mira-type variables (Scholz 1992). Single Mira-type variables can usually produce many strong emission lines in their spectra (Merrill 1960; Fox et al. 1984), e.g. the FeII lines. On the other hand, the broad Balmer lines and the forbidden lines of the oxygen originates from the circumbinary material.

5 CONCLUSIONS

We obtained high-resolution optical spectroscopy and X-ray observations of the D-type symbiotic star EF Aql. Using the spectra and additional photometry, we estimated the temperature ($T_{hot} \sim 55\,000$ K) and the luminosity ($L_{hot} \sim 5.3 L_{\odot}$) of the hot component in the system. The measured parameters of the emission lines in the spectra, reveal possible ionization potential dependent stratification. We performed periodogram analysis on the available V-band photometric data and found an improved period of 320.4 ± 0.3 d, which is the period of pulsations of the Mira-type donor star.

The *Swift* observation did not detect EF Aql in X-rays. The upper limit of the X-ray observations is 0.003 c s^{-1} which, for a δ -type spectrum, corresponds into an unabsorbed flux of $10^{-12} \text{ erg cm}^{-2} \text{ s}^{-1}$. This means that EF Aql may well be comparable to the X-ray faintest δ -type symbiotics detected so far. However, we detected EF Aql in the UV with an average UVM2 magnitude of 14.05. Based on IR data, we estimate the distance to EF Aql to be ~ 3.1 kpc and a mass-loss rate of the Mira donor of $\sim 2.5 \times 10^{-7} M_{\odot} \text{ yr}^{-1}$. The optical and X-ray observations point that EF Aql is an accretion-powered symbiotic star without shell burning. The results are proof that the D-type symbiotic stars deserve more attention and observations, which can help to understand the binary companions to asymptotic giant branch (AGB) stars and their evolution.

ACKNOWLEDGEMENTS

We thank the anonymous referee for the comments which improved the paper. This work is supported by the grant KII-06-H28/2 08.12.2018 (Bulgarian National Science Fund). The paper is based on spectroscopic observations made with the Southern African Large Telescope (SALT) under programme 2018-1-MLT-005 (PI: J. Mikołajewska). Polish participation in SALT is funded by grant No. MNiSW DIR/WK/2016/07. This research has been partly funded by the National Science Centre, Poland, through grant OPUS 2017/27/B/ST9/01940 to J. Mikołajewska. GJML is a member of the CIC-CONICET (Argentina) and acknowledge support from grant ANPCYT-PICT 0901/2017. J. Martí acknowledges support by Agencia Estatal de Investigación grant AYA2016-76012-C3-3-P from the Spanish Ministerio de Economía y Competitividad (MINECO), and by Consejería de Economía, Innovación, Ciencia y Empleo of Junta de Andalucía under research group FQM-322, as well as FEDER funds.

We thank Brad Cenko, the PI of the *Neil Gehrels Swift* observatory, for a general allocation of observing time. This research has made use of the NASA/IPAC Infrared Science Archive, which is operated by the Jet Propulsion Laboratory, California Institute of Technology, under contract with the National Aeronautics and Space Administration and the XRT Data Analysis Software (XRTDAS) developed under the responsibility of the ASI Science Data Center (ASDC), Italy. The authors acknowledge the variable star observations from the AAVSO International Database contributed by observers worldwide and used in this research. ASAS-SN is supported by the Gordon and Betty Moore Foundation through grant GBMF5490 to the Ohio State University and NSF grant AST-1515927. Development of ASAS-SN has been supported by NSF grant AST-0908816, the Mt. Cuba Astronomical Foundation, the Center for Cosmology and AstroParticle Physics at the Ohio State University, the Chinese Academy of Sciences South America Center for Astronomy (CAS-SACA), the Villum Foundation, and George Skestos.

REFERENCES

- Allen D. A., 1982, Infrared studies of symbiotic stars.. pp 27–42
- Ballester P., 1992, in European Southern Observatory Conference and Workshop Proceedings. p. 177
- Bramall D. G., et al., 2010, The SALT HRS spectrograph: final design, instrument capabilities, and operational modes. p. 77354F
- Bramall D. G., et al., 2012, The SALT HRS spectrograph: instrument integration and laboratory test results. p. 84460A
- Buckley D. A. H., Swart G. P., Meiring J. G., 2006, Completion and commissioning of the Southern African Large Telescope. p. 62670Z
- Crause L. A., et al., 2014, Performance of the Southern African Large Telescope (SALT) High Resolution Spectrograph (HRS). p. 91476T
- Crawford S. M., et al., 2010, PySALT: the SALT science pipeline. p. 773725
- Davidson A., Malina R., Bowyer S., 1977, *ApJ*, **211**, 866
- Fox M. W., Wood P. R., Dopita M. A., 1984, *ApJ*, **286**, 337
- Friedjung M., Mikołajewska J., Zajczyk A., Eriksson M., 2010, *A&A*, **512**, A80
- Gromadzki M., Mikołajewska J., Whitelock P., Marang F., 2009, *Acta Astron.*, **59**, 169

- Gromadzki M., Mikołajewska J., Soszyński I., 2013, *Acta Astron.*, **63**, 405
- Hinkle K. H., Fekel F. C., Joyce R. R., Wood P., 2013, *ApJ*, **770**, 28
- Höfner S., Olofsson H., 2018, *A&ARv*, **26**, 1
- Jura M., 1994, *ApJ*, **422**, 102
- Kalirai J. S., Marigo P., Tremblay P.-E., 2014, *ApJ*, **782**, 17
- Kniazev A. Y., Gvaramadze V. V., Berdnikov L. N., 2017, *SALT Spectroscopy of Evolved Massive Stars*. p. 480
- Kochanek C. S., et al., 2017, *PASP*, **129**, 104502
- Kotnik-Karuza D., Friedjung M., Exter K., Keenan F. P., Pollacco D. L., Whitelock P. A., 2004, *New results about dust in the envelope of the symbiotic nova RR Tel*. pp 363–366
- Kuranov A. G., Postnov K. A., 2015, *Astronomy Letters*, **41**, 114
- Le Bertre T., Tanaka M., Yamamura I., Murakami H., 2003, *A&A*, **403**, 943
- Luna G. J. M., Sokoloski J. L., Mukai K., Nelson T., 2013, *A&A*, **559**, A6
- Lutz J. H., Kaler J. B., Shaw R. A., Schwarz H. E., Aspin C., 1989, *PASP*, **101**, 966
- Margon B., Prochaska J. X., Tejos N., Monroe T., 2016, *PASP*, **128**, 024201
- Merrill P. W., 1960, *Spectra of Long-Period Variables*. p. 509
- Mikołajewska J., 2012, *Baltic Astronomy*, **21**, 5
- Mikołajewska J., Acker A., Stenholm B., 1997, *A&A*, **327**, 191
- Muerst U., Nussbaumer H., Schmid H. M., Vogel M., 1991, *A&A*, **248**, 458
- Munari U., Patat F., 1993, *A&A*, **277**, 195
- Munari U., Zwitter T., 1997, *A&A*, **318**, 269
- Murset U., Nussbaumer H., 1994, *A&A*, **282**, 586
- Netzer H., 1975, *MNRAS*, **171**, 395
- Neugebauer G., et al., 1984, *ApJ*, **278**, L1
- O’Donoghue D., et al., 2006, *MNRAS*, **372**, 151
- Orio M., Zezas A., Munari U., Siviero A., Tepedelenlioglu E., 2007, *ApJ*, **661**, 1105
- Paczynski B., Zytkov A. N., 1978, *ApJ*, **222**, 604
- Peterson B. M., 1997, *An Introduction to Active Galactic Nuclei*
- Pojmanski G., 1997, *Acta Astron.*, **47**, 467
- Reinmuth K., 1925, *Astronomische Nachrichten*, **225**, 385
- Richwine P., Bedient J., Slater T., Mattei J. A., 2005, *Journal of the American Association of Variable Star Observers (JAAVSO)*, **34**, 28
- Roberts D. H., Lehar J., Dreher J. W., 1987, *AJ*, **93**, 968
- Schmid H. M., 1989, *A&A*, **211**, L31
- Scholz M., 1992, *A&A*, **253**, 203
- Shappee B., et al., 2014, in *American Astronomical Society Meeting Abstracts #223*. p. 236.03
- Sokoloski J. L., Bildsten L., Ho W. C. G., 2001, *MNRAS*, **326**, 553
- Stahl O., Kaufer A., Tubbesing S., 1999, *The FEROS spectrograph*. p. 331
- Stellingwerf R. F., 1978, *ApJ*, **224**, 953
- Trabucchi M., Wood P. R., Montalbán J., Marigo P., Pastorelli G., Girardi L., 2019, *MNRAS*, **482**, 929
- Vassiliadis E., Wood P. R., 1993, *ApJ*, **413**, 641
- Webster B. L., Allen D. A., 1975, *MNRAS*, **171**, 171
- Whitelock P., Menzies J., Feast M., Marang F., Carter B., Roberts G., Catchpole R., Chapman J., 1994, *MNRAS*, **267**, 711
- Whitelock P., Marang F., Feast M., 2000, *MNRAS*, **319**, 728
- Whitelock P. A., Feast M. W., van Loon J. T., Zijlstra A. A., 2003, *MNRAS*, **342**, 86
- Whitelock P. A., Feast M. W., Van Leeuwen F., 2008, *MNRAS*, **386**, 313
- Woitke P., 2006, *A&A*, **460**, L9
- Zamanov R. K., et al., 2017, *Astronomische Nachrichten*, **338**, 680

This paper has been typeset from a $\text{\TeX}/\text{\LaTeX}$ file prepared by the author.